

Article

# Delay Equivalences in Tuning PID Control for the Double Integrator Plus Dead-Time

Mikulas Huba <sup>1,\*</sup>  and Damir Vrancic <sup>2</sup> 

<sup>1</sup> Faculty of Electrical Engineering and Information Technology, Institute of Automotive Mechatronics, Slovak University of Technology, 812 19 Bratislava, Slovakia

<sup>2</sup> Department of Computer Automation and Control, J. Stefan Institute, SI-1000 Ljubljana, Slovenia; damir.vrancic@ijs.si

\* Correspondence: mikulas.huba@stuba.sk; Tel.: +421-905-524-357

**Abstract:** The paper investigates and explains a new simple analytical tuning of proportional-integrative-derivative (PID) controllers. In combination with  $n$ th order series binomial low-pass filters, they are to be applied to the double-integrator-plus-dead-time (DIPDT) plant models. With respect to the use of derivatives, it should be understood that the design of appropriate filters is not only an implementation problem. Rather, it is also critical for the resulting performance, robustness and noise attenuation. To simplify controller commissioning, integrated tuning procedures (ITPs) based on three different concepts of filter delay equivalences are presented. For simultaneous determination of controller + filter parameters, the design uses the multiple real dominant poles method. The excellent control loop performance in a noisy environment and the specific advantages and disadvantages of the resulting equivalences are discussed. The results show that none of them is globally optimal. Each of them is advantageous only for certain noise levels and the desired degree of their filtering.

**Keywords:** filtration; multiple real dominant pole method; PID control; derivative action



**Citation:** Huba, M.; Vrancic, D. Delay Equivalences in Tuning PID Control for the Double Integrator Plus Dead-Time. *Mathematics* **2021**, *9*, 328. <https://doi.org/10.3390/math9040328>

Academic Editors: Libor Pekař and Radek Matušů

Received: 11 January 2021

Accepted: 2 February 2021

Published: 7 February 2021

**Publisher's Note:** MDPI stays neutral with regard to jurisdictional claims in published maps and institutional affiliations.



**Copyright:** © 2021 by the authors. Licensee MDPI, Basel, Switzerland. This article is an open access article distributed under the terms and conditions of the Creative Commons Attribution (CC BY) license (<https://creativecommons.org/licenses/by/4.0/>).

## 1. Introduction

The range of methods suitable for controlling time-delayed systems is very large and growing (see, e.g., [1–7]). A particular area of interest concerns higher-order (HO) generalizations of traditional proportional-integral-derivative (PID) control. This motivation follows from the intensive research in fractional-order PID (FO-PID) control [8]. In this concept, the non-integer derivative and integrative solutions are in the end approximated by HO filters. In contrast, in the concept of  $PID_n^m$  control [9,10] (generalized PID control with  $m$ th-order derivatives and  $n$ th-order low-pass filters), possibly including controllers with HO derivatives such as proportional-integral-derivative-accelerative (PIDA) control [11–16], the HO controllers are designed directly. As the main motivation for the FO-PID control, one can say that one tries to find more degrees of freedom. These should be used to specify the resulting control performance, robustness and measurement noise attenuation [8,10]. Mostly, application areas are mentioned in which the acquisition of a more detailed plant model is not possible or not reasonable. In particular, these are areas that are extremely attractive because even small improvements in performance result in large economic gains: e.g., vehicle attitude control when driving on a road with a variable profile, control of highly nonlinear robotic systems and load frequency control of power plants. In this context, all these innovative solutions are typically implemented by embedded controllers. Before extending the design to controllers with HO derivatives and to controlled systems approximated by second-order time-delay models, it seems useful to show and analyze its essence and problems using the example of a PID controller with first-order derivatives.

An example of the control system under consideration is shown in Figure 1. Here,  $y$  represents the plant output,  $r$  the reference setpoint,  $u$  the control signal (manipulated variable),  $d_i$  an input disturbance and  $\delta$  a measurement noise. The task of control loop design is not only to find the parameters of the control blocks  $C(s)$  and the low-pass filter  $Q_n(s)$  to suppress the measurement noise, but may also involve the selection of the most appropriate model of the system  $F(s)$ . It is often advantageous to work with the simplest possible model  $F(s)$  and to include all resulting inaccuracies and uncertainties of the plant modeling in the acting disturbance  $d_i$ .

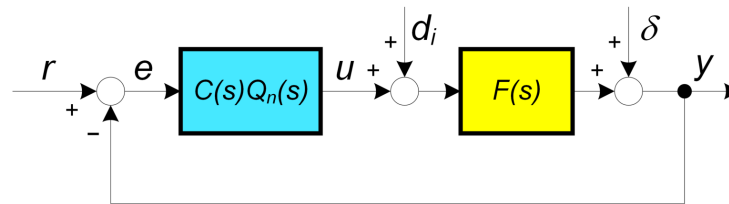


**Figure 1.** Considered control loop with an output  $y$ , a reference setpoint  $r$ , an input disturbance  $d_i$  and a measurement noise  $\delta$ . The possibly improper PID controller with transfer function  $C(s)$  is combined with a low-pass filter  $Q_n(s)$  and the plant model  $F(s)$ .

For the approximation of more complex real plant dynamics (models based on first-order time-delayed systems are commonly used to control simpler (lower-order) systems [2]), the double integrator plus dead time (DIPDT) model

$$F(s) = K_s e^{-T_d s} / s^2 \quad (1)$$

will be used. Note that model (1) also represents the simplest possible second order process transfer function. Additionally, the total dead-time  $T_d$  may consist of an estimate of the plant delay  $T_m$  (which includes, for example, an actuator dead-time  $T_a$  and a communication delay  $T_c$ ) and an intentionally introduced equivalent filter delay estimate  $T_e$ .

$$T_d = T_m + T_e \quad (2)$$

In this work,  $T_e$  is used to approximate dynamics of the low-pass filters  $Q_n(s)$  required in terms of implementing and achieving sufficiently smooth and robust transients.

Note that the estimated plant gain substituted for  $K_s$  in controller tuning is  $K_m$ .

DIPDT models have already been used in the work [17,18] to design constraint controllers for potentially unstable higher order plants. Motivations for working with DIPDT models are well described, for example, in [19]. In [20] the “half rule” was presented, which allows one to obtain a simplified DIPDT model of the plant even from a more complex plant transfer function. The advantages of “ultra-local” integral models (1) are also widely used in the so-called model-free control [21]. Although they can be expected to achieve a required accuracy only in the close neighborhood of an operating point, they are preferred because of their simplicity and easier identification. Purely integral models are also behind “active disturbance rejection control” (ADRC), which is based on linear extended state observer (LESO) [22–24]. ADRC approximates the potentially complex and nonlinear feedback dynamics by an additional state corresponding to an equivalent input disturbance, and fuses external and internal disturbances corresponding to modeling uncertainties. The possible combination of ADRC with dead time compensation is considered in [4,5].

This paper develops further the results of the design of the HO-PID controller, which focus on the control of systems approximated by the integrator-plus-dead-time (IPDT) models [10] and the conference paper [25], which compares the controller design for DIPDT systems using the performance portrait method with the multiple real dominant poles method.

The rest of the paper is organized as follows. Section 2 presents the performance measures used and their applications in optimal controller design. Section 3 deals with

the optimal PID controller tuning using the multiple real dominant poles (MRDP) method. Tuning considering the unavoidable implementation and noise reduction filters is described in Section 4. Section 5 introduces the simulation experiments proposed to check properties of the different time delay equivalents used to tune the filters. The main results of the work are evaluated in Section 6 followed by the Discussion in Section 7 and summarized in the Conclusions, along with suggestions for possible further research.

## 2. Time and Shape Related Performance Measures

One of the main drawbacks of numerous optimal control methods is that they narrow the problem to evaluating the speed of transients. Among the many different alternatives [26,27], this can be quantified as the settling time, integral of squared error (ISE), or more frequently [28], using the integral of the absolute error (IAE).

$$IAE = \int_0^{\infty} |e(t)| dt ; r = w - y , \quad (3)$$

Here,  $r$  can be a piecewise constant reference setpoint,  $y$  the plant output and  $e$  the control error. However, IAE-based controller optimization usually leads to a global optimum with a slight overshoot of the output, which is not acceptable in numerous applications. For the sake of brevity, this paper only addresses the evaluation of the behavior with respect to the input disturbance steps. It should be noted that any inaccuracy of the model manifests itself as equivalent input disturbance. Therefore, such an evaluation is also crucial for the case of reference setpoint steps.

Since IAE-optimal control can also lead to reduced robustness, additional optimization constraints must be applied. These are predominantly represented by peaks in the maximum sensitivity and complementary sensitivity functions ( $M_s$  and  $M_t$ ). Although the use of sensitivity functions is widespread, we are driven to replace them by several serious reasons:

- (a) **No connection to real-time control:** by evaluating data obtained from experiments on real processes, we cannot determine the actual values of the sensitivity functions;
- (b) **Unsuitability for unstable systems:** when controlling unstable systems, we are not content with the recommended ranges  $M_s \in [1.2, 2]$  (suitable only for controlling stable systems) [27], but the required values may be much higher (see, for example, [29], who recommends  $M_s \approx 10$ , or [30], who works even with  $M_s \approx 20$ );
- (c) **Potential counterproductivity:** in terms of robust control design, the use of sensitivity functions can lead to counterproductive results [10].

In this work, they are replaced by more effective [10] shape-based constraints.

### 2.1. Monotonicity-Based Shape Related Measures

Often, whether the author explicitly declares it or not, we are interested in smooth transient shapes. The question, however, is how we can quantify their smoothness in order to account for them. On the other hand, the history of using shape-based constraints is very long. Already Ziegler and Nichols [31] worked with quarter-amplitude-damping in their seminal work defining shape constraints for the disturbance response. In the era of relay time optimal control of  $n$ th-order systems, the requirement to terminate the process in  $n$  (rectangular) control intervals was used dominantly. It was first formulated in work by Feldbaum [32] and later modified by the formulated maximum/minimum principle [33] only for the case of complex poles of the system and a large distance between the initial and final states. Although the relay time optimal controllers disappeared from the literature over time (with some exceptions such as [34], which continued to use Feldbaum's theorem on  $n$  intervals of control), the shape requirements appeared in a different form in the formulation of the dead-beat behavior of linear discrete responses [35]. However, despite this clear historical evidence, the use of shape-based performance measures can be considered neglected. The works [26,27] in this direction represent one of the first attempts to unify all previous usages.

Moreover, although also not always used in controller design, the need to limit the total control effort measured, for example, by the total input variation (TV, [20]), is well known. The value TV, defined as the sum of the absolute values of all signal increments, depends dominantly on the shape of the signal under consideration. The drawback of working with a performance measure TV is that it presents unstructured information: the “useful” control interventions required to achieve the control objective are mixed with excessive interventions resulting from model or measurement inaccuracies. Therefore, in the work [26], it was proposed to use modified criteria based on deviations of a given transient from monotonicity instead of the performance measure TV. Monotonicity is not only one of the fundamental mathematical concepts, but also closely related to several important physical properties and the shape of control transients.

Although the other derived performance measures are primarily intended for the evaluation of quasi-continuous-time responses, we consider evaluation with digital computers in the derived formulas. However, we consider the sampling period to be short enough not to affect the evaluations. Based on TV, a modified performance measure  $TV_0(y)$  works with samples  $y_i, i \in [0, \infty)$  obtained from the signal  $y(t)$  with an initial value  $y_0$  and a final value  $y_\infty$ , whereby

$$TV_0(y) = \sum_{i=0}^{\infty} |y_{i+1} - y_i| - |y_\infty - y_0| \tag{4}$$

$TV_0(y)$  can be interpreted as a deviation from monotonicity.  $TV_0(y) = 0$  only for monotonic (non-increasing or non-decreasing) responses  $y(t)$ . Otherwise  $TV_0(y) > 0$ .

To further combine the requirement of monotonicity with the Feldbaum’s theorem and its modification for smooth signal transients, we recall that the inversion of the dynamics of a simple integrator implies that the monotone output transient requires an input signal consisting of two monotone intervals [36]. Similarly, when considering dynamics inversion for higher order integrators, it may be useful to introduce the notion of  $n$ -pulse ( $nP$ ) function.

**Definition 1** ( $nP$  function  $u(t)$ ). Consider a function of time  $u(t)$  that is continuous for  $t \in [0, T], T > 0$ , with possible discontinuity at  $t = 0^+$  and with initial value  $u_0 = u(0^-)$  and final value  $u_T = u(T)$ . Suppose that for  $t > 0$  there are at least  $n$  extreme points satisfying

$$\begin{aligned} u_{m,i} = u(t_{m,i}) \notin [u_0, u_T]; \quad i = 1, 2, \dots, n \text{ for } 0 < t_{m,1} < \dots < t_{m,n} \\ (u_{m,i} - u_T) (u_{m,i+1} - u_T) < 0; \quad i = 1, 2, \dots, n - 1 \end{aligned} \tag{5}$$

If  $u(t)$  is monotonic on each interval that does not contain one of these extreme points  $u_{m,i}$ ,  $u(t)$  is called an  $n$ -Pulse ( $nP$ ) function. By allowing discontinuity at  $t = 0$ , the first extreme point can also move to  $t = 0^+$ , shrinking the first monotonic interval before this extreme point to zero. Following this terminology, the monotonic transients can also be referred to as  $0P$  and the periodic responses as  $\infty P$  functions.

In this way, we have unified the terminology based on shape requirements for a wide range of piecewise monotonic responses, which include the oscillatory loop transients. On this basis, it is then possible to design performance measures based on deviations from  $nP$  shapes, which we obtain by applying (4)  $n$  times.

For a one-pulse ( $1P$ ) shape [36] consisting of two monotonic intervals separated by an extreme point  $y_m \notin (y_0, y_\infty)$  lying outside the interval formed by the initial and final output values  $y_0$  and  $y_\infty$ , the deviations from an ideal  $1P$  behavior summarize the deviations from monotonicity on these two intervals:

$$TV_1(y) = \sum_i |y_{i+1} - y_i| - |2y_m - y_\infty - y_0| \tag{6}$$

The computation of  $TV_1(y)$ , which is essentially used to evaluate disturbance step responses in this paper, requires finding the extreme point lying outside the strip  $y \in (y_0, y_\infty)$ .

In the case of multiple extreme points, the maximum deviation must be chosen as  $y_m$ .

Geometrically, an ideal 2P input shape of a piece-wise continuous control signal  $u(t), t \in [0^-, \infty)$  is specified by two extreme points  $u_{m1}, u_{m2}$  that occur at times  $t_1, t_2 \in (0, \infty)$ , lie between the initial and final values  $u_0$  and  $u_\infty$  and satisfy

$$(u_{m1} - u_\infty)(u_{m2} - u_\infty) < 0 \quad (7)$$

Ideally, these extreme points separate the control signal into three monotonic control intervals. If there are multiple extreme points, again the extreme points must satisfy (7) and all less important other extreme points can be neglected. Excessive control effort can then be evaluated by summing up the deviations from monotonicity on these three intervals according to

$$TV_2(u) = \sum_i (|u_{i+1} - u_i|) - |2u_{m1} - 2u_{m2} + (u_\infty - u_0)\text{sign}(u_{m1} - u_\infty)| \quad (8)$$

**Remark 1** (Fundamental difference from traditional optimization). *As mentioned above, simultaneously with the shape of the transients, we also try to optimize the speed of the transients. Since in this work, the requirement of the bounded total control effort is refined by minimizing the excessive control effort (exceeding the unavoidable acceleration and deceleration during the input step responses), this focus is one of the most important differences from the traditional quadratic optimal control, which is concerned with minimizing the total controller activity. It can also be considered as one of the cornerstones of the success of the presented approaches.*

When evaluating responses restricted to the step changes of the input disturbance  $d_i$  (since all model uncertainties of the system appear as disturbances [37], the optimization of the disturbance behavior is also important for optimal setpoint tracking of systems with uncertain models), leading to one-pulse (1P) transients at the plant output and two-pulse (2P) transients at the input (given by the inversion of the plant model dynamics [38,39]), we will use TV modified to evaluate deviations from these shapes.

## 2.2. Optimization Problem

Different cost functions and different optimization constraints have already been defined and used for loop optimization. A loop optimization that requires a fast output with minimal excessive control effort, as measured by the shape-related deviations, can search for a minimal value of the cost function

$$J_k(u) = IAE^k TV_2(u) \quad (9)$$

To achieve a fast output but with minimal output wobbling, the disturbance response cost function can be modified to

$$J_k(y) = IAE^k TV_1(y) \quad (10)$$

By using a different exponent  $k$ , it is possible to define a different weight ratio of the speed of transients and the considered shape deviations within the optimization.

The trade-off between the speed of the control transients and the shape-related deviations at the input and output can be represented by different types of characteristics. They can be based on above two cost functions, thereby expressing effect of a chosen tuning parameter.

## 2.3. Speed-Effort and Speed-Wobbling Characteristics

In order to relate the shape-related deviations at the input with the speed of the control deviation (IAE), we can define the speed-effort characteristic curve (SE). Thereby, the excessive control effort measured in terms of  $TV_2(u)$  will be considered as the variable

$\zeta$ . The speed of the control error attenuation (*IAE*) will be considered as the variable  $\eta$  and the characteristic parameter may be chosen as the equivalent filter delay  $T_e$ .

Similarly, to relate excessive output wobbling to *IAE*, the speed-wobbling (*SW*) characteristic may be used. Its variable  $\zeta$  will then be represented by  $TV_1(y)$  (for the disturbance steps), when

$$\begin{aligned} SE : \zeta &= TV_2(u), \eta = IAE, \text{ or} \\ SW : \zeta &= TV_1(y), \eta = IAE \end{aligned} \tag{11}$$

### 3. PID Controller According to the MRDP Method

The history of the multiple real dominant poles (MRDP) method dates back to one of the first textbooks in control engineering [40], which cites even older sources on the subject used to design simple controllers. To this day, many authors resort to it (see, e.g., [41–43] and the references therein, but the requirement of the double real dominant pole is also found in the SIMC method [20]). The essence of this method is to find the controller setting that gives multiple real dominant (stable) poles in the closed loop. By analyzing simpler control loops, e.g., with a P controller and an integrator-plus-dead-time (IPDT) system [44], it can be shown that a multiple real pole represents the limiting case between the existence of oscillatory transients corresponding to a complex pole pair and the existence of different real poles leading to slower and faster transient modes. Since the resulting transient speed is determined by a slower mode, the optimal setting again corresponds to a compromise represented by the multiple real poles. The existence of the searched solution must be ensured by an appropriate choice of the controller structure. The multiplicity of the sought poles must ensure a sufficient number of equations to determine the controller parameters. We achieve the dominance of multiple poles in the presence of several possible roots by choosing the slowest stable solution.

The initial steps of writing this paper were inspired by the modified (improved) SIMC controller [19,20]. Some preliminary results dedicated to the position servo control were published in [45]. This work focuses on the analysis of the influence of different equivalences of time delays used in setting the controllers, with respect to the low-pass filters used. The MRDP approach first deals with the setting of an ideal PID controller.

**Definition 2** (Ideal PID controller). *By an ideal PID controller we will understand the controller given by the improper transfer function*

$$C(s) = \frac{U(s)}{E(s)} = K_c \left( 1 + \frac{1}{sT_i} + sT_D \right) \tag{12}$$

whereby  $K_c$  is the controller gain,  $T_i$  the integral and  $T_D$  the derivative time constant.

We cannot directly implement such a controller, but its concept simplifies further considerations. From the closed loop transfer functions corresponding to the feedback combination of the ideal controller (12) and DIPDT plant (1) we get (with  $Q_n(s) = 1$  in Figure 1) the transfer functions

$$\begin{aligned} F_{r0}(s) &= \frac{Y(s)}{R(s)} = \frac{K_c K_m (1 + T_i s + T_i T_D s^2)}{T_i s^3 e^{T_d s} + K_c K_m (1 + T_i s + T_i T_D s^2)} \\ F_i(s) &= \frac{Y(s)}{D_i(s)} = \frac{K_m T_i s}{T_i s^3 e^{T_d s} + K_c K_m (1 + T_i s + T_i T_D s^2)} \end{aligned} \tag{13}$$

**Theorem 1** (Optimal controller tuning). *For the parameters  $T_d > 0, K_m \neq 0$  of the model (1), the “optimal” controller parameters  $K_{co}, T_{io}$  and  $T_{Do}$  guaranteeing a quadruple real dominant pole (QRDP)  $s_0$  of the characteristic quasi-polynomial*

$$P(s) = T_i s^3 e^{T_d s} + K_c K_m (1 + T_i s + T_i T_D s^2) \tag{14}$$

may be expressed by dimensionless (normed) parameters  $\kappa_o$ ,  $\tau_{i_o}$  and  $\tau_{D_o}$  as

$$\begin{aligned} \kappa_o &= K_{co}K_mT_d^2 = 0.125 \\ \tau_{i_o} &= T_{i_o}/T_d = 10.324 \\ \tau_{D_o} &= T_{D_o}/T_d = 4.043 \end{aligned} \tag{15}$$

**Proof.** The required pole multiplicity results from the number of unknown parameters of the controller (three), to which the unknown value  $s_o$  is added. To guarantee a quadruple pole,  $s_o$  has to fulfill conditions

$$\left[ P(s); \frac{dP(s)}{ds}; \frac{d^2P(s)}{ds^2}; \frac{d^3P(s)}{ds^3} \right]_{s=s_o} = \mathbf{0} \tag{16}$$

From  $d^3P(s)/ds^3 = T_i e^{T_d s} (6 + 18T_d s + 9s^2 T_d^2 + s^3 T_d^3) = 0$  we get roots

$$s_1 = -0.416/T_d; s_2 = -2.294/T_d; s_3 = -6.290/T_d \tag{17}$$

The dominant pole is the solution which is the closest to the imaginary axis and thus corresponds to the slowest stable transients, i.e.,  $s_o = s_1$ . □

**Definition 3** (Low-pass filters). For implementation and to achieve an appropriate noise filtration, the ideal controller (12) (see Figure 1) will be combined with a series binomial low-pass filter  $Q_n(s)$

$$Q_n(s) = \frac{1}{(T_f s + 1)^n}; n = 1, 2, \dots \tag{18}$$

For a given sampling period  $T_s$  used for a quasi-continuous-time control implementation,  $T_f$  has to be chosen to fulfill  $T_s \ll T_f$ .

#### 4. Equivalent Delay Based Controller Tuning

The application of the control requires solving several problems:

- The ideal PID controller may not be realized—to be causal, it must be extended by at least a first-order low-pass filter (18);
- A more effective attenuation of the measurement noise can be achieved by the filter order  $n > 1$ ;
- The included filters  $Q_n(s)$  modify the loop dynamics, which must be taken into account in the controller tuning.

A direct application of the MRDP method to control loops containing the filter dynamics in combination with the dead-time leads to complex formulas that are usually analytically incomprehensible. Therefore, similar to [10,20,46], simplified approaches based on replacing the filter transfer function by an equivalent dead time  $T_e$  that can be simply added to the identified system delay  $T_m$  (2) are used. This requires the use of the following approach:

1. After identifying the system model parameters  $K_m$  and  $T_m$ , select an appropriate value of the tuning parameter  $T_e > 0$  corresponding to the required degree of filtration;
2. Specify the controller parameter (15) corresponding to the total loop delay  $T_d$  (2);
3. Select a filter order  $n$  and specify the filter time constant  $T_f$  by a suitable delay equivalence described below, defined as

$$T_f/T_e = f(n) \tag{19}$$

4. Check that the computed value  $T_f$  satisfies the requirement  $T_f \gg T_s$  in (18), where  $T_s$  represents the sampling period used for the quasi-steady control implementation.
5. If not, either decrease  $T_s$ , or  $n$ , which must still fulfill the condition  $n \geq 1$ .

6. By experimentally evaluating the noise attenuation characteristics for different  $n$ , choose an optimal controller that guarantees the optimal control loop performance.

4.1. Half-Rule Equivalence (HRE)

A simple delay equivalence was proposed by Skogestad [20] in the form of a “half rule.” When applied to the filter (18) in combination with the integrating plant model (1) it may be expressed as

$$T_f/T_e = f_{HRE} = 2/n \tag{20}$$

4.2. Average Residence Time Equivalence (ARTE)

ARTE is based on the comparison of areas bounded by the normalized unit step response of the filter and the asymptote to its steady-state value [47]. It can be expressed as

$$T_f/T_e = f_{ARTE} = 1/n \tag{21}$$

4.3. Dominant Poles Equivalence (DPE)

The closed-loop transfer functions considering the double integrator plant in combination with  $Q_n(s)$ ,  $T_d = 0$  and ideal PID control (12) lead to the characteristic polynomial

$$P_n(s) = T_i s^3 (1 + T_f s)^n + K_c K_s (1 + T_i s + T_i T_D s^2) \tag{22}$$

In denoting its roots as  $s_n$ , the requirement of an equal position of the two considered multiple real dominant poles

$$s_o = s_n, \quad n = 1, 2, 3, \dots \tag{23}$$

an equivalence between the time constants  $T_f$  and the equivalent dead time  $T_d$  considered in (15) is obtained. The corresponding values  $T_f/T_e = f_{DPE}$  can be found in Table 1.

**Table 1.** PID control: equivalent time delay ratios  $f(n) = T_f/T_e, n \in [1, 7]$ .

$n$	1	2	3	4	5	6	7
$f_{HRE}$	2	1	0.667	0.5	0.4	0.333	0.286
$f_{ARTE}$	1	0.5	0.333	0.25	0.2	0.167	0.143
$f_{DPE}$	0.601	0.373	0.271	0.213	0.176	0.149	0.130

Numerically, the comparison with the HRE (20) and ARTE (21) shows significant differences that need to be verified by simulation. Here, the resulting IAE values (whether the equivalence leads to an overly conservative loop tuning) and the shape deviations at the input and output (whether excessively oscillating transients occur) must be compared, e.g., with the cost Functions (9) and (10).

**5. Evaluation of the Results**

In order to explain all the details important for practical applications, idealized shapes undistorted by noise should be analyzed prior to considering realistic noise applications for the vector of the tuning parameters:

$$T_e = \{0.02, 0.05, 0.2, 0.4, 0.8, 1.5, 3.0, 5.0\} T_d \tag{24}$$

$$n \in [1, 5]$$

As the differences between the individual equivalences are observable only for larger  $T_e$  values, the visualization in Figure 2 shows just a reduced sample of the analyzed responses corresponding to

$$T'_e = \{0.4, 0.8, 1.5, 3.0, 5.0\}T_d \quad (25)$$

$$n \in [1, 5]$$

They document that for all values of the tuning parameter, DPE yields nearly ideal 1P step responses at the output and 2P step responses at the input. Especially for shorter  $T_e$ , the responses corresponding to the different values of  $n$  are very close to each other. Therefore, from a practical point of view, they can be considered equivalent.

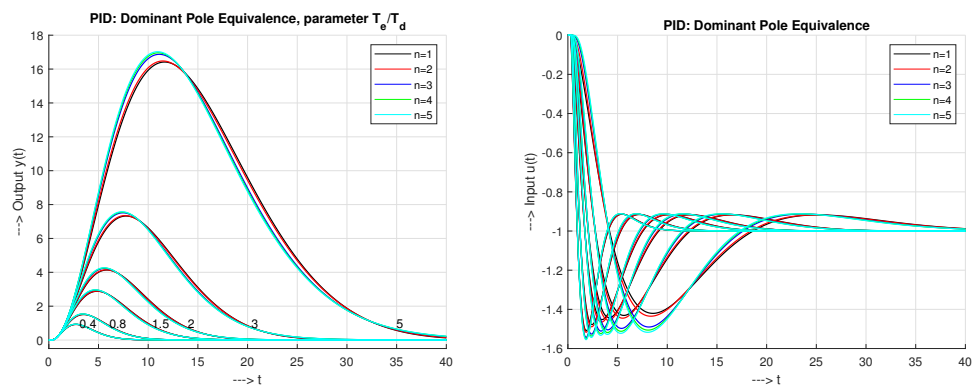


Figure 2. Dominant pole equivalence: input disturbance step responses corresponding to parameters (25), no noise.

A similar set of input disturbance step responses corresponding to HRE (Figure 3) shows that this equivalence yields much more oscillatory and only slowly damped transients, at least for longer equivalent delays.

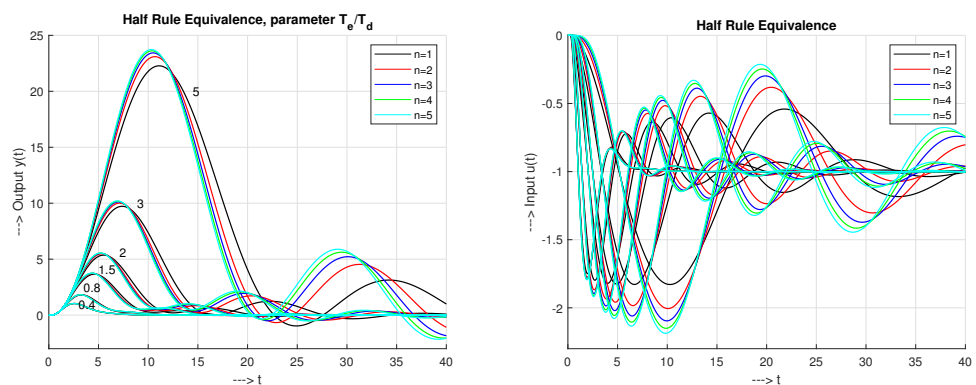


Figure 3. Half rule equivalence: input disturbance step responses corresponding to parameters (25), no noise.

Finally, ARTE shows results almost equivalent to DPE, with homogeneous shapes of the responses over the whole set of  $T_e$  values considered (Figure 4) and with only slightly increased maximum amplitude of the disturbance step responses. Visually, the differences between the responses corresponding to the different values of  $n$  are even smaller than for DPE.

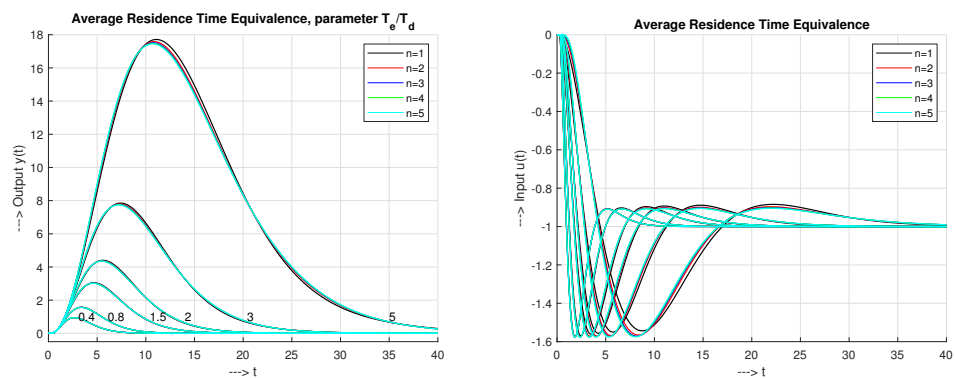


Figure 4. Average residence time equivalence: input disturbance step responses corresponding to parameters (25), no noise.

5.1. Holistic Cost Functions versus Equivalent Delay

Without measurement noise, the combined cost functions as functions of  $T_e$  (Figure 5 above) increase much faster with increasing  $T_e$  for HRE than for DPE and ARTE. The introduction of measurement noise (Figure 5 middle) significantly changes not only the shapes of the characteristics, but also their vertical distribution: the DPE characteristics, which were lowest without noise consideration, rise above the other two characteristics when noise is taken into account; for the HRE characteristics, the situation is reversed in the range of smaller  $T_e$  values. The use of higher order filters significantly increases noise attenuation. To illustrate the influence of noise amplitude, we can repeat the same analyzes again for  $T_e$  values (24) with significantly increased  $|\delta| \leq 0.2$ . It can be seen from Figure 5 that the inflection points with the optima of the cost functions  $J(u)$  and  $J(y)$  shift slightly to higher  $T_e$  values, without any significant change in the characteristics.

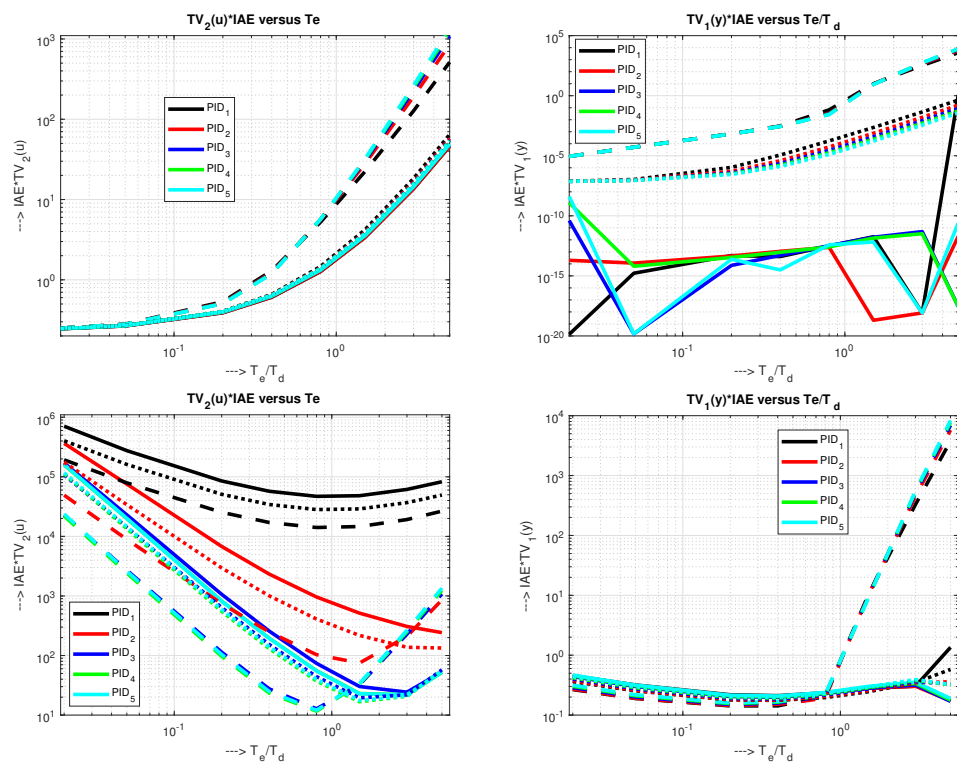
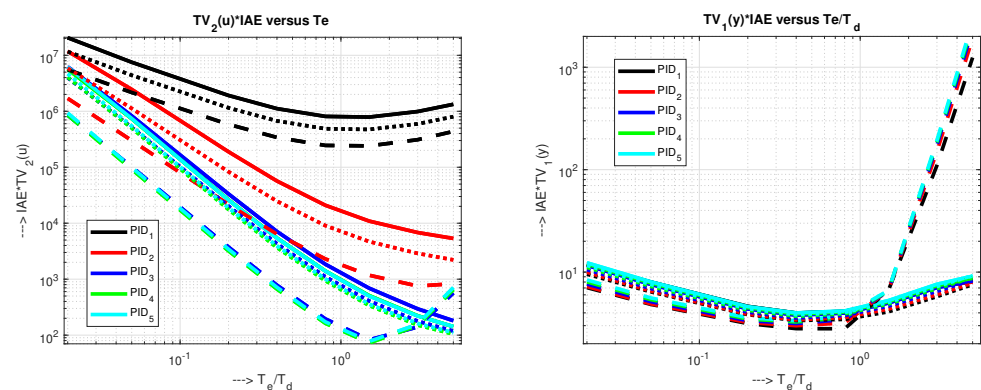


Figure 5. Cont.



**Figure 5.** Cost Functions (9) (left) and (10) (right) as functions of the equivalent time  $T_e$  (25),  $n \in [1, 5]$ ; DPE (full curves), HRE (dashed) and ARTE (dotted); no noise (above), noise  $|\delta| \leq 0.01$  (middle) and  $|\delta| \leq 0.2$  (below);  $k = 1$ .

The experience gained can be summarized in the conclusion that while DPE leads to the most advantageous dependencies of the combined functions  $J_u$  and  $J_y$  on  $T_e$  in loops without measurement noise, the opposite is true in loops with measurement noise. The most advantageous properties, but only in a limited range of  $T_e$  values, are given by HRE. If it is nevertheless necessary to work with relatively large values of  $T_e$ , ARTE must be used.

### 5.2. Interpretation Is SE/SW Planes

The comparison of individual equivalences or the suitability of the selection of filter parameters is made possible by the features fo SE and SW characteristics. The following requirements can be formulated for their use.

**Remark 2** (Performance requirements in SE and SW planes). *For the least possible excessive effort or wobbling, the operating points corresponding to some  $T_e$  should be as left as possible in the SE and SW planes [10]. At the same time, they should be as low as possible for the fastest possible transients.*

In this sense, in terms of excessive control effort, filters with  $n = 1$  (see Figure 6) represent the worst solution. Their SE characteristics are located furthest to the right. The excessive control effort can be significantly reduced by choosing  $n = 2$ . Significant improvements can still be achieved by  $n \geq 3$ . Here, HRE provides the least excessive effort for the relatively short  $T_e$  values and the relatively high speed of transients (specified by low IAE). However, for longer  $T_e$  values with higher IAE, the excessive effort may actually increase (due to the control imperfections). The inflection point in the HRE performance is even better seen in the SW -characteristics. Here the choice of filter order has a much smaller impact. These conclusions regarding the SE and SW characteristics hold without significant changes for both lower ( $|\delta| < 0.01$ ) and higher ( $|\delta| < 0.2$ ) noise amplitudes.

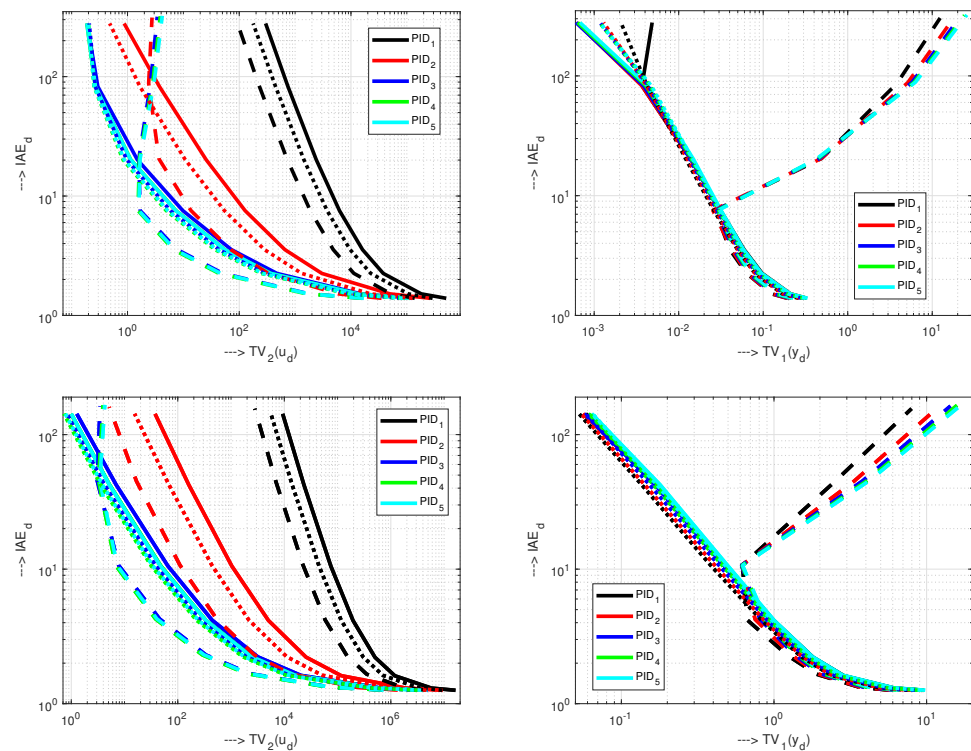


**Figure 6.** Speed-effort (SE) (left) and speed-wobbling (SW) characteristics (right) corresponding for  $T_e$  (25) to DPE (full curves), HRE (dashed) and ARTE (dotted); noise  $|\delta| < 0.01$  (above) and  $|\delta| < 0.2$  (below);  $k = 1$ .

## 6. Discussion

The analysis of individual delay equivalences has shown that, in an idealized loop, the dominant-pole-equivalence (DPE) gives the best results, being generally more accurate than the average-residence-time-equivalence (ARTE) and the half-rule-equivalence (HRE). However, the differences obtained are largely lost compared to measurement noise. Thus, excellent results can be obtained with a simple HRE known for many years. However, this is only true for filter delays that do not exceed a certain threshold. Above this the loop characteristics deteriorate severely. Therefore, for a wide choice range of  $T_e$  values, working with ARTE can be recommended.

## 7. Conclusions and Future Work

The paper has shown that analytical tuning of PID controllers for time delayed double integrator systems may be reliably applied in a wide range of filter delays and noise amplitudes. The method retains its simplicity by including possible additional dynamic loop elements (series filters) in an equivalent delay added to the identified system delay. In doing so, it can easily include other inertial elements of the loop.

The detailed analysis we performed of the control of the DIPDT system by PID controllers opens the way to the control of this system with the use of higher order controllers and the generalization of some preliminary results from [16,25]. This also makes various applications possible, similarly to the control of first-order time-delayed systems [10,45]. However, before that, some issues concerning the design of controllers with two degrees of freedom [41–43] with the optimization of transients after setpoint steps and the issues of a suitable anti-windup and bumpless transfer [10,47] have to be resolved.

**Author Contributions:** Writing—original draft preparation, M.H. and D.V.; simulations, M.H.; editing, D.V. and M.H.; project administration, M.H. All authors have read and agreed to the published version of the manuscript.

**Funding:** This research was funded by the grants APVV SK-IL-RD-18-0008 Platoon Modeling and Control for mixed autonomous and conventional vehicles: a laboratory experimental analysis; VEGA 1/0745/19, Control and modeling of mechatronic systems in emobility; and within research program P2-0001, financed by the Slovenian Research Agency.

**Acknowledgments:** Supported by E-Academia Slovaca, non-profit organization, Sadmeljská 1, 831 06 Bratislava, Slovakia.

**Conflicts of Interest:** The authors declare no conflict of interest.

## Abbreviations

The following abbreviations are used in this manuscript:

1P	One-Pulse, response with 2 monotonic segments (1 extreme point)
2P	Two-Pulse, response with 3 monotonic segments (2 extreme points)
ADRC	Active Disturbance Rejection Control
DIPDT	Double Integrator Plus Dead-Time
FO	Fractional Order
HO	Higher Order
IAE	Integral Absolute Error
IPDT	Integrator Plus Dead-Time
ISE	Integral Square Error
LESO	Linear Extended State Observer
MRDP	Multiple Real Dominant Pole
nP	n-Pulse, response with $n + 1$ monotonic segments ( $n$ extreme points)
PID	Proportional-Integrative-Derivative
$PID_n^m$	generalized PID with $m$ th order derivative action and $n$ th order low-pass filter
SE	Speed-Effort
SW	Speed-Wobbling
TV	Total Variation
$TV_0$	Deviation from monotonicity (0P shape)
$TV_1$	Deviation from 1P shape
$TV_2$	Deviation from 2P shape

## References

- Richard, J.P. Time-delay systems: An overview of some recent advances and open problems. *Automatica* **2003**, *39*, 1667–1694. [[CrossRef](#)]
- O'Dwyer, A. *Handbook of PI and PID Controller Tuning Rules*, 3rd ed.; Imperial College Press: London, UK, 2009.
- O'Dwyer, A. An Overview of Tuning Rules for the PI and PID Continuous-Time Control of Time-Delayed Single-Input, Single-Output (SISO) Processes. In *PID Control in the Third Millennium. Lessons Learned and New Approaches*; Vilanova, R., Visioli, A., Eds.; Springer: Berlin/Heidelberg, Germany, 2012.
- Chen, S.; Xue, W.; Zhong, S.; Huang, Y. On comparison of modified ADRCs for nonlinear uncertain systems with time delay. *Sci. China Inf. Sci.* **2018**, *61*, 70223. [[CrossRef](#)]
- Zhao, S.; Gao, Z. Modified active disturbance rejection control for time-delay systems. *ISA Trans.* **2014**, *53*, 882–888. [[CrossRef](#)]
- Pekař, L. On Simple Algebraic Control Design and Possible Controller Tuning for Linear Systems with Delays. *Int. J. Mech.* **2018**, *12*, 178–191.
- Pekař, L.; Gao, Q. Spectrum Analysis of LTI Continuous-Time Systems With Constant Delays: A Literature Overview of Some Recent Results. *IEEE Access* **2018**, *6*, 35457–35491. [[CrossRef](#)]
- Tepljakov, A.; Alagoz, B.B.; Yeroğlu, C.; Gonzalez, E.; HosseinNia, S.H.; Petlenkov, E. FOPID Controllers and Their Industrial Applications: A Survey of Recent Results. *IFAC Pap.* **2018**, *51*, 25–30. [[CrossRef](#)]
- Huba, M.; Vrančić, D.; Bisták, P.  $PID_n^m$  Control for IPDT Plants. Part 1: Disturbance Response. In Proceedings of the 26th Mediterranean Conference on Control and Automation (MED), Zadar, Croatia, 19–22 June 2018.
- Huba, M.; Vrančić, D.; Bisták, P. PID Control with Higher Order Derivative Degrees for IPDT Plant Models. *IEEE Access* **2020**, *9*, 2478–2495. [[CrossRef](#)]
- Jung, S.; Dorf, R.C. Novel Analytic Technique for PID and PIDA Controller Design. *IFAC Proc. Vol.* **1996**, *29*, 1146–1151. [[CrossRef](#)]
- Ukakimaparn, P.; Pannil, P.; Boonchuay, P.; Trisuwannawat, T. PIDA Controller designed by Kitti's Method. In Proceedings of the 2009 ICCAS-SICE, Fukuoka City, Japan, 18–21 August 2009; pp. 1547–1550.
- Guha, D.; Roy, P.K.; Banerjee, S. Multi-verse optimisation: a novel method for solution of load frequency control problem in power system. *IET Gener. Transm. Distrib.* **2017**, *11*, 3601–3611. [[CrossRef](#)]

14. Kumar, M.; Hote, Y.V. Robust CDA-PIDA Control Scheme for Load Frequency Control of Interconnected Power Systems. *IFAC Pap.* **2018**, *51*, 616–621. [[CrossRef](#)]
15. Kumar, M.; Hote, Y.V. Robust PIDD2 Controller Design for Perturbed Load Frequency Control of an Interconnected Time-Delayed Power Systems. *IEEE Trans. Control. Syst. Technol.* **2020**, 1–8. [[CrossRef](#)]
16. Huba, M. Filtered PIDA Controller for the Double Integrator Plus Dead Time. In Proceedings of the 16th IFAC International Conference on Programmable Devices and Embedded Systems, High Tatras, Slovakia, 29–31 October 2019.
17. Huba, M.; Bisták, P.; Skachová, Z.; Žáková, K. P- and PD-Controllers for  $I_1$  and  $I_2$  Models with Dead Time. In Proceedings of the 6th IEEE Mediterranean Conference on Control and Automation, Sardinia, Italy, 9–11 June 1998; Volume 11, pp. 514–519.
18. Huba, M.; P.Bisták, Z.; Žáková, K. Predictive Antiwindup PI and PID-Controllers Based on  $I_1$  and  $I_2$  Models with Dead Time. *IEEE Mediterr. Conf.* **1998**, *11*, 532–535.
19. Grimholt, C.; Skogestad, S. Optimal PID control of double integrating processes. *IFAC Pap.* **2016**, *49*, 127–132. [[CrossRef](#)]
20. Skogestad, S. Simple analytic rules for model reduction and PID controller tuning. *J. Process. Control.* **2003**, *13*, 291–309. [[CrossRef](#)]
21. Fliess, M.; Join, C. Model-free control. *Int. J. Control.* **2013**, *86*, 2228–2252. [[CrossRef](#)]
22. Han, J. From PID to Active Disturbance Rejection Control. *Ind. Electron. IEEE Trans.* **2009**, *56*, 900–906. [[CrossRef](#)]
23. Gao, Z. Active disturbance rejection control: A paradigm shift in feedback control system design. In Proceedings of the American Control Conference, Minneapolis, MN, USA, 14–16 June 2006; pp. 2399–2405.
24. Gao, Z. On the centrality of disturbance rejection in automatic control. *ISA Trans.* **2014**, *53*, 850–857. [[CrossRef](#)]
25. Huba, M.; Škrinářová, J.; Dudáš, A.; Bisták, P. Optimal PID controller tuning for the time delayed double integrator. In Proceedings of the 21st International Carpathian Control Conference—ICCC, Starý Smokovec, Slovak Republic, 27–29 May 2020.
26. Huba, M. Designing Robust Controller Tuning for Dead Time Systems. In *International Conference on System Structure and Control*; IFAC: Ancona, Italy, 2010.
27. Huba, M. Performance Measures and the Robust and Optimal Control Design. In Proceedings of the 3rd IFAC Conference on Advances in Proportional-Integral-Derivative Control, Ghent, Belgium, 9–11 May 2018; pp. 960–965.
28. Shinskey, F. How good are Our Controllers in Absolute Performance and Robustness. *Meas. Control.* **1990**, *23*, 114–121. [[CrossRef](#)]
29. Begum, K.G.; Rao, A.S.; Radhakrishnan, T. Maximum sensitivity based analytical tuning rules for PID controllers for unstable dead time processes. *Chem. Eng. Res. Des.* **2016**, *109*, 593–606. [[CrossRef](#)]
30. Boskovic, M.C.; Sekara, T.B.; Rapaic, M.R. Novel tuning rules for PIDC and PID load frequency controllers considering robustness and sensitivity to measurement noise. *Int. J. Electr. Power Energy Syst.* **2020**, *114*, 105416. [[CrossRef](#)]
31. Ziegler, J.G.; Nichols, N.B. Optimum settings for automatic controllers. *Trans. ASME* **1942**, *11*, 759–768. [[CrossRef](#)]
32. Feldbaum, A. *Optimal Control Systems*; Academic Press: New York, NY, USA, 1965.
33. Pontrjagin, L.; Boltjanskij, V.; Gamkrelidze, R.; Miščenko, J. *The Mathematical Theory of Optimal Processes*; Interscience: New York, NY, USA, 1962.
34. Föllinger, O. *Regelungstechnik. 8. Auflage*; Hüthig Buch Verlag: Heidelberg, Germany, 1994.
35. Kuo, B. *Discrete-Data Control Systems*; Prentice-Hall: Upper Saddle River, NY, USA, 1970.
36. Huba, M. Performance measures, performance limits and optimal PI control for the IPDT plant. *J. Process. Control.* **2013**, *23*, 500–515. [[CrossRef](#)]
37. Chen, W.H.; Yang, J.; Guo, L.; Li, S. Disturbance-Observer-Based Control and Related Methods—An Overview. *IEEE Trans. Ind. Electron.* **2016**, *63*, 1083–1095. [[CrossRef](#)]
38. Huba, M.; Šimuněk, M. Modular Approach to Teaching PID Control. *IEEE Trans. Ind. Electr.* **2007**, *54*, 3112–3121. [[CrossRef](#)]
39. Huba, M. Open flexible PD-controller design for different filtering properties. In Proceedings of the 39th Annual Conference of the IEEE Industrial Electronics Society (IECON), Vienna, Austria, 10–13 November 2013.
40. Oldenbourg, R.; Sartorius, H. *Dynamik Selbsttätiger Regelungen*, 2nd ed.; R.Oldenbourg-Verlag: München, Germany, 1951.
41. Vítečková, M.; Víteček, A. 2DOF PI and PID controllers tuning. In Proceedings of the 9th IFAC Workshop on Time Delay Systems, Prague, Czech Republic, 7–9 June 2010; Volume 9, pp. 343–348.
42. Vítečková, M.; Víteček, A. 2DOF PID controller tuning for integrating plants. In Proceedings of the 2016 17th International Carpathian Control Conference (ICCC), High Tatras, Slovakia, 29 May–1 June 2016; pp. 793–797.
43. Viteckova, M.; Vitecek, A.; Janacova, D. Robustness and Multiple Dominant Pole Method. In Proceedings of the 2020 21th International Carpathian Control Conference (ICCC), Star Smokovec, Slovak Republic, 27–29 October 2020; pp. 1–4.
44. Huba, M. Comparing 2DOF PI and Predictive Disturbance Observer Based Filtered PI Control. *J. Process. Control.* **2013**, *23*, 1379–1400. [[CrossRef](#)]
45. Bélai, I.; Huba, M.; Burn, K.; Cox, C. PID and filtered PID control design with application to a positional servo drive. *Kybernetika* **2019**, *55*, 540–560. [[CrossRef](#)]
46. Huba, M. Filter choice for an effective measurement noise attenuation in PI and PID controllers. In Proceedings of the ICM2015, Nagoya, Japan, 6–8 March 2015.
47. Åström, K.J.; Hägglund, T. *Advanced PID Control*; ISA: Research Triangle Park, NC, USA, 2006.